Journal of Theoretical and Applied Information Technology
28th February 2013. Vol. 48 No.3
© 2005 - 2013 JATIT & LLS. All rights reserved·
ISSN: 1992-8645 www.jatit.org E-ISSN: 1817-3195

A NEW GEAR FAULT RECOGNITION METHOD USING MUWD SAMPLE ENTROPY AND GREY INCIDENCE

[1]WENBIN ZHANG, [2]JIE MIN, [3]YASONG PU

[1]Assoc Prof., College of Engineering, Honghe Univ., Mengzi, Yunnan, 661100, China

[2]Lecturer, College of Engineering, Honghe Univ., Mengzi, Yunnan, 661100, China

[3]Lecturer, College of Engineering, Honghe Univ., Mengzi, Yunnan, 661100, China

E-mail: [1]georgezwb@sohu.com, [2]77713541@qq.com, [3]377821053@qq.com

ABSTRACT

In this paper, we propose a new gear fault recognition method by using morphological undecimated wavelet decomposition (MUWD), sample entropy and grey incidence. MUWD possesses both the characteristic of morphological filter in morphology and multi-resolution in wavelet transform. Then we develop multi-scale MUWD based on the characteristic of impulse feature extraction in difference morphological filter. At first, we use multi-scale MUWD to process different gear fault signals in five levels, signal length is maintained invariable and information loss could be avoided in MUWD, simulation example tests the good effectiveness of its denoising capacity. Second, we calculate the sample entropy of each level. Different fault type corresponds with different sample entropy. In the end, we serve sample entropy as the feature vectors and calculate the grey incidence of different gear vibration signals to identify the fault pattern and condition. Practical example shows that the high efficiency of the proposed method. It is suitable for condition monitoring and fault diagnosis of gear.

Keywords: *Morphological Undecimated Wavelet Decomposition (MUWD), Grey Incidence, Sample Entropy (SE), Recognition, Fault Diagnosis, Gear*

1. INTRODUCTION

Gear is the common used part in mechanical transformation, their carrying capacity and reliability being prominent for the overall machine performance. Therefore, the fault recognition of gear has been the subject of extensive research. Enveloping analysis and wavelet packages decomposition are common used fault feature extraction methods for gear signal [1]. But the enveloping analysis needs to confirm the center frequency and frequency band of band-pass filter; it will impact the analyzing results [2]. While the wavelet decomposition has finite length of basic function, energy will leak in the signal processing. Due to the wavelet decomposition that is based on the linear decomposition, so the good effectiveness will not be obtained in processing gear fault data because of the non-linear and non-stationary behaviors.

Proposed by Goutisias and Heijmans [3-4] in 2000, the morphological wavelet is a non-linear wavelet transformation based on mathematical morphology. Morphological wavelet possesses both the characteristic of feature recognition and multi-resolution in wavelet transform; it also has good details keeping and noise resisting abilities. Study of morphological wavelet in 1-D vibration signal is starting step by step [5]. However, the traditional wavelet adopts a decimated wavelet decomposition method; information will be lost in decomposition procedures. Literature [6] firstly proposed a morphological undecimated wavelet decomposition method based on undecimated wavelet scheme. Then a new morphological undecimated wavelet decomposition method is proposed and used in gear fault diagnosis [7-8].

Gear fault signal is the typical non-stational and non-linear signal. How to extract feature parameter of different fault pattern is the key for gear fault diagnosis. Sample entropy is a good tool to evaluate complexity of non-linear time series, compared with other existing non-linear dynamic methods; it has many good characteristic, such as good residence of noise

© 2005 - 2013 JATIT & LLS. All rights reserved·
ISSN: 1992-8645 www.jatit.org E-ISSN: 1817-3195

interference, closer agreement with theory for data sets with known probabilistic content. Moreover, sample entropy displays the property of relative consistency in situations where approximate entropy does not [9]. These performances are suitable for fault extraction in practice.

The arrangement of the paper is as follows. Introduction elaborates in section-1. Section-2 describes elaborately the concepts of morphological filter and coupled wavelet, section-3 gives the definition of sample entropy, section-4 introduces the definition of grey incidence, the proposed methodology is explained in section 5, section 6 and section 7 give the simulation and practical application of the proposed method and finally, the conclusion is given in section 8.

2. BASIC CONCEPTS OF MORPHOLOGICAL FILTER AND COUPLED WAVELET

Morphological Filter. A morphological filter is constructed by different morphological transforms. Dilation and erosion are two basic morphological transforms. While dilation is the transform used to expand the target object and shrink the hole, erosion is the transform used to shrink the target object and expand the hole. Let $f(x)$ and $g(\mathbf{x})$ denote 1-D input signal and structure element, where $F=\{0, 1, \ldots, N\text{-}1\}$ and $G=\{0, 1, \ldots, M\text{-}1\}$ denote sets on which signal f and g are defined, $N \geq M$. Dilation and erosion of f and g are thus defined as follows

$$(f \oplus g)(n) = \max_{m=0,1,\cdots,M-1} \{f(n-m)+g(m)\}. \quad (1)$$

$$(f \ominus g)(n) = \min_{m=0,1,\cdots,M-1} \{f(n+m)-g(m)\}. \quad (2)$$

$$(n=0,1,\ldots,N-M)$$

$$(n=0,1,\ldots,N+M-2)$$

Where $\oplus$ denotes dilation transform and $\ominus$ denotes erosion transform.

Usually, dilation and erosion are not mutual inverse. They can be combined through cascade connection to form new transforms. If dilation is next to erosion, such cascade transform is an opening transform. The contrary is a closing transform. The transforms can be computed using the following formulas respectively

$$(f\circ g)(n)=[f\ominus g\oplus g](n). \quad (3)$$

$$(f\cdot g)(n)=[f\oplus g\ominus g](n). \quad (4)$$

Where $\circ$ denotes opening transform and $\cdot$ denotes closing transform.

The opening and closing results of the signal f by the elliptical structure element g are shown in figure 1 [10].

(a) *opening and its result*

(b) *closing and its result*

Fig1. Opening And Closing Results Of The Signal F By The Elliptical Structure Element G.

From figure 1(a), when g moves under f closely, the parts of f that do not contact with g will fall into the upper edge of g. So the opening transform can be used to remove the peaks in the signal. From Figure 1(b), when g moves over f closely, the parts of f that do not contact with g will roll into the lower edge of g. So the closing transform can be used to fill the valleys in the signal. Both transforms can be combined to form a morphological filter because they have the capacity of low-pass filtering.

Principle of difference morphological filter. In morphological operations, open and close operations have different processing performances. Open operation could restrain positive impulse and keep negative impulse, while close operation will have inverse functions. So in the practical application, we should select relative morphological operation corresponding with processing aim. But sometimes it is difficult to get transcendental knowledge of practical positive and negative impulses; the universal situation is that the positive and negative impulses are contained in practical data at the same time [11]. Therefore, it is necessary to construct morphological filtering algorithm with combination of open and close operations. The definition of difference morphological filter is

$$DIF(f)=f\cdot g-f\circ g. \quad (5)$$

Journal of Theoretical and Applied Information Technology
28th February 2013. Vol. 48 No.3
© 2005 - 2013 JATIT & LLS. All rights reserved·
ISSN: 1992-8645 www.jatit.org E-ISSN: 1817-3195

From equation (5) we can see that the difference morphological filter may be used to extract the impulsive components of the signal. The reason is shown in equation (6).

$$f \bullet g - f \circ g = (f \bullet g - f) + (f - f \circ g). \quad (6)$$

Here, $f \bullet g - f$ and $f - f \circ g$ operations are two forms of morphology Top-Hat transform. The former operation is called black Top-Hat transformation, which is used to extract negative impulse; while the latter is called white Top-Hat transformation, which is used to extract positive impulse. So the different morphological filter could extract the positive and negative impulses at the same time.

Principle of coupled wavelet decomposition. The synthesis and analysis operators must satisfy the pyramid condition which plays an important role in constructing the operators of the decomposition scheme. Consider a family V_j of signal spaces where j is a finite or an infinite index set. Here the signals consist of two families of operators, a family $\psi_j^{\uparrow}$ of analysis operators mapping V_j into V_{j+1} and a family $\Psi_j^{\downarrow}$ of synthesis operators mapping V_{j+1} back into V_j. The analysis and synthesis operators $\psi_j^{\uparrow}$, $\Psi_j^{\downarrow}$ are said to satisfy the pyramid condition if $\psi_j^{\uparrow}\Psi_j^{\downarrow} = \mathrm{id}$ on V_{j+1} where id is an identity operator. The pyramid condition guarantees that no information is lost in two consecutive steps: synthesis and analysis. It is the fundamental principle used to construct pyramid and wavelet operators.

The coupled wavelet is constructed according to the pyramid condition. A coupled wavelet comprises of two analysis operators and one synthesis operator. The analysis operators include a signal analysis operator and a detail analysis operator. Figure 2 shows the coupled wavelet decomposition scheme. In Figure 2, V_j and W_j are two sets: V_j is the signal space at level j and W_j is the detail space at level j: $\psi_j^{\uparrow}: V_j \rightarrow V_{j+1}$ is the signal analysis operator, $\omega_j^{\uparrow}: V_j \rightarrow W_{j+1}$ is the detail analysis operator and $\Psi_j^{\downarrow}$ is the synthesis operator mapping the information back to the lower level. In order to guarantee that no information is lost and the decomposition is non-redundant, the analysis operators $\psi_j^{\uparrow}$, $\omega_j^{\uparrow}$ and synthesis operator $\Psi_j^{\downarrow}$ of the coupled wavelet must satisfy the pyramid condition below

$$\psi_j^{\uparrow}(\Psi_j^{\downarrow}(x,y)) = x, \quad \text{if } x \in V_{j+1}, y \in W_{j+1}. \quad (7)$$

$$\omega_j^{\uparrow}(\Psi_j^{\downarrow}(x,y)) = y, \quad \text{if } x \in V_{j+1}, y \in W_{j+1}. \quad (8)$$

In order to yield a complete signal representation, the maps $(\psi_j^{\uparrow}, \omega_j^{\uparrow}): V_j \rightarrow V_{j+1} \times W_{j+1}$ and $\Psi_j^{\downarrow}: V_{j+1} \times W_{j+1} \rightarrow V_j$ are the inverses of each other. This leads to the following perfect reconstruction condition

$$\Psi_j^{\downarrow}(\psi_j^{\uparrow}(x), \omega_j^{\uparrow}(x)) = x, \quad \text{if } x \in V_j. \quad (9)$$

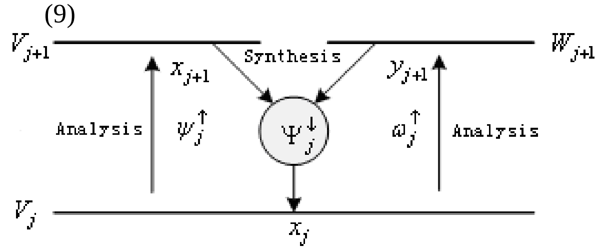

Fig2. Coupled Wavelet Decomposition Scheme.

The coupled wavelet provides a standard structure for the multi-resolution signal decomposition schemes. Based on this structure, the MUWD scheme is presented by regenerating the analysis operators and synthesis operators [8].

3. DEFINITION OF SAMPLE ENTROPY

Let $[x(n)]=x(1), x(2), \ldots, x(N)$ denotes N-elements time series representing gear vibration signal. Then, the estimation algorithm of sample entropy consists of the following steps [12-13]:

(i) creating of m vectors defined as:

$$X_m(i)=[x(i), x(i+1), \ldots, x(i+m-1)]. \quad (10)$$

$$(i=1, 2, \ldots, N-m+1).$$

(ii) calculation of a distance between two vectors in the following way:

$$d[X_m(i), X_m(j)] = \max_{k=0,\cdots,m-1} |x(i+k)-x(j+k)|. \quad (11)$$

(iii) calculation of number of similar segments in two vectors:

$nm = \#\, d[X_m(i), X_m(j)] \le r$, while $i \ne j$;

$nm+1 = \#\, d[X_{m+1}(i), X_{m+1}(j)] \le r$, while $i \ne j$.

where r is a tolerance parameter

Journal of Theoretical and Applied Information Technology
28th February 2013. Vol. 48 No.3
© 2005 - 2013 JATIT & LLS. All rights reserved·
ISSN: 1992-8645 www.jatit.org E-ISSN: 1817-3195

(iv) calculation of similarity measures of these segments:

$$B_i^m(r)=\frac{1}{N-m+1}n_m.$$

$$A_i^m(r)=\frac{1}{N-m+1}n_{m+1} \quad \text{while } i=1,\ldots,N\text{-}m.$$

(v) calculation of mean measures of the similar signal segments:

$$B^m\frac{\sum_{i=1}^{N-m}B_i^m(r)\cdot}{N-m} \qquad A^m=\frac{\sum_{i=1}^{N-m}A_i^m(r)\cdot}{N-m}$$

(vi) calculation of sample entropy estimation

$$\text{Samp-En}(m,r)=-\ln\frac{A^m(r)}{B^m(r)}. \qquad (12)$$

4. GREY INCIDENCE

According to the grey theory, the relation degree evolves from the relation coefficient. The relation coefficient of the two series X_i and X_j, is represented by $\zeta_{ij}(k)$, where k represents the sampling points [14-15].

$$\Delta_{ij}(k)=|X_j(k)\text{-}X_i(k)|k\in\{1,2,\cdots N\}.$$
(13)

$$\Delta\text{min}=\min_j\min_k\Delta_{ij}(k)$$

$$\Delta\text{max}=\max_j\max_k\Delta_{ij}(k)$$

$\zeta_{ij}(k)$ is defined as:

$$\xi_{ij}=\frac{\Delta_{\min}+\Delta_{\max}\cdot\rho}{\Delta_{ij}(k)+\Delta_{\max}\cdot\rho} \qquad k\in\{1,2,\cdots N\}.$$

(14)

Where ρ is a constant with the range from 0 to 1. The value of ρ determines the classification capacity and is usually recommended to be 0.5. The relation degree of the two series X_i and X_j is as following:

$$\xi_{ij}=\frac{1}{N-1}\cdot\frac{1}{2}[\sum_{k=1}^{N}\xi_{ij}(k)+\sum_{k=2}^{N-1}\xi_{ij}(k)] \quad .$$

(15)

The relation degree represented by ζ_{ij} shows the comparability of the X_i and X_j series. It is often applied to grey cluster in practice [16]. Obviously, the bigger ζ_{ij} is, the greater the inference of X_i to X_j would be.

5. GEAR FAULT RECOGNITION METHOD

In order to extract gear fault feature, let ϕ represent morphological closing operator and γ represent opening operator. Based on the MUWD scheme proposed by literature [6], we construct a new MUWD method for fault feature extraction. It is shown that

$$x_{j+1}=y_j^{\cdot}(x_j)=f(x_j,(j+1)g_0)\text{-}\ g(x_j,(j+1)g_0) \quad . \qquad (16)$$

$$y_{j+1}=w_j^{\cdot}(x_j)=\text{id}\text{-}[f(x_j,(j+1)g_0)\text{-}\ g(x_j,(j+1)g_0)] \quad . \qquad (17)$$

$$\Upsilon_j^{-}(y_j^{\cdot}(x_j),w_j^{\cdot}(x_j))=y_j^{\cdot}(x_j)+w_j^{\cdot}(x_j)=x_j \quad . \qquad (18)$$

Equation (10) represents processing signal x_j with structure element $(j+1)g_0$ by selecting multi-scale difference morphological filtering. In which, $(j+1)g_0$ denotes the dilation operation for j times with structure element g_0. The approximate signal from equation (10) represents the impulsive feature by difference morphological filter with different scale structure elements [8].

Using the grey relation degree to identify fault, the first step is to build standard fault feature matrix. Assume the number of typical faults is k, and each typical fault contains one feature vector which is constructed by some feature parameters. Then a standard fault feature matrix could be constructed by these feature vectors. The second step is to assume there are some groups of pending series, and a pending series feature matrix could be constructed. The third step is to calculate the grey similar relation degree between the pending series feature matrix and each typical fault by using equation (15).

Set the standard fault feature matrix is $[X_{ri}]$:

Journal of Theoretical and Applied Information Technology
28th February 2013. Vol. 48 No.3
© 2005 - 2013 JATIT & LLS. All rights reserved·
ISSN: 1992-8645 www.jatit.org E-ISSN: 1817-3195

$$X_{ri}=\begin{bmatrix} X_{r1} \\ X_{r2} \\ \vdots \\ X_{rn} \end{bmatrix} = \begin{bmatrix} X_{r1}(1) & X_{r2}(2) & \cdots & X_{r1}(k) \\ X_{r2}(1) & X_{r2}(2) & \cdots & X_{r2}(k) \\ \vdots & \vdots & \cdots & \vdots \\ X_{rn}(1) & X_{rn}(2) & \cdots & X_{rn}(k) \end{bmatrix}. \quad (19)$$

Here, r refers to the standard fault feature vector, n refers to the number of the standard fault feature vector, and k refers to the dimension of each standard fault feature vector.

Let the jth pending fault feature vector is

$$[X_{tj}]=[X_{tj}(1),X_{tj}(2),\ldots,X_{tj}(k)]. \quad (20)$$

Then the grey relation degree rank will be

$$[\xi_{tjri}]=[\xi_{tjr1},\xi_{tjr2},\ldots,\xi_{tjrn}]. \quad (21)$$

According to the biggest principle of relation degree, set $\xi_{tjrm}(m=1,2,\ldots,n)$ is the biggest one, the potential fault type could correspond with m [14].

The detailed steps of this algorithm as follows:

(i) The original signal is decomposed by morphological undecimated wavelet decomposition into different levels.

(ii) We calculate the sample entropy of each level with equation (12) and then we get a set of fault feature matrix.

(iii) We build the standard fault feature matrix from the calculated data.

(iv) The grey relation between the symptom set and standard fault set is calculated as the identification evidence.

6. SIMULATION

To verify the effectiveness of the new MUWD scheme on noise suppression and impulsive feature extraction, the simulated signal is formulated as follows [8]:

$$x(t)=7x_1(t)+0.7x_2(t)+i(t). \quad (22)$$

Here, $x_1(t)$ is a typical series of exponentially decaying impulses with the impulse function of $f(t)=e^{-25t\sin(25\pi t))}$ and the impulse frequency of 16Hz; $x_2(t)$ is the sum of two harmonic waves: $x_2(t)=\cos(2\pi\times20t)+\cos(2\pi\times40t)$; $i(t)$ is the Gauss white noise with the standard deviation of 1. Figure 3 shows the waveform in time domain and spectrums of the simulated signal and the impulse components.

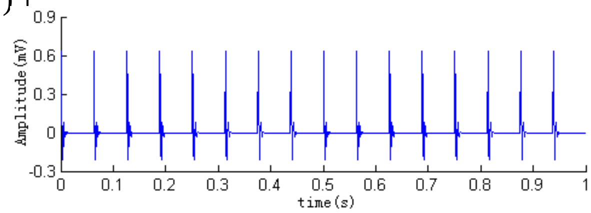

(A) Waveform In Time Domain Of Impulse Signal

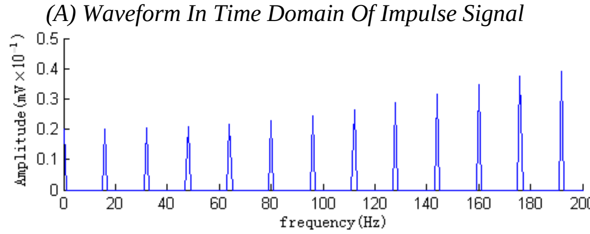

(B) Spectrum Of The Impulse Signal

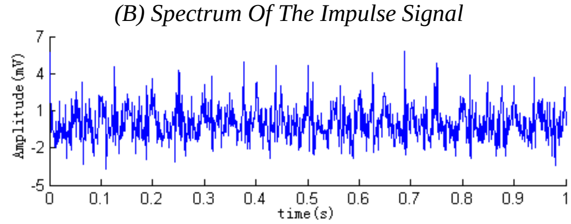

(C) Waveform In Time Domain Of Simulated Signal

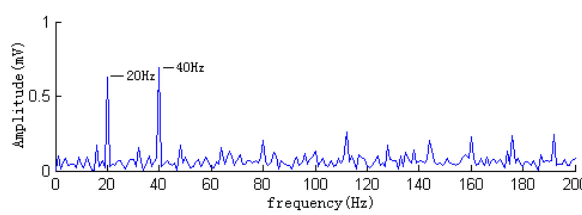

(D) Spectrum Of Simulated Signal

Fig3. Waveforms In Time Domain And Spectrums Of Impulse Signal And Simulated Signal.

Figure 3(d) is the partially enlarged spectrum of the signal, from which the harmonic waves of 25 and 50 Hz are obvious, while the impulse components can not be seen clearly because it mixes with the harmonic waves and Gauss white noise. In order to stand out the impulsive feature, the harmonic waves and noises must be suppressed.

Insert the flat structure element $g_0=\{0,0,0\}$ into equation (16)-(18), the new MUWD

© 2005 - 2013 JATIT & LLS. All rights reserved·
ISSN: 1992-8645 www.jatit.org E-ISSN: 1817-3195

procedure was applied to the simulated signal using two levels of analysis operation. Figure 4 shows the approximate signal and its spectrum in second level. From it we can see the firstly three orders of the impulse frequencies. It is shown that the new MUWD method has good effectiveness in impulsive feature extraction.

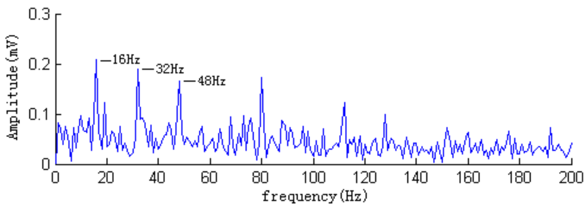

Fig4. Spectrum Of Simulated Signal After New MUWD.

7. PRACTICAL EXAMPLE

To verify good effectiveness in fault recognition, all vibration signals were collected from the experimental testing of gearbox using the accelerometer which was mounted on the outer surface of the bearing case of input shaft of the gearbox [17-19]. The speed of the motor is 1420 RPM and the sample frequency is 16384 Hz. The four conditions were tested that were normal, slight-worn, medium-worn, broken-teeth. Now we get five sampled data sets of each condition. First, we use MUWD method to process the original signal in five levels. Figure 5(a) shows the spectrum of the original broken-teeth signal. Figure 5(b) shows the processed signal in the first level.

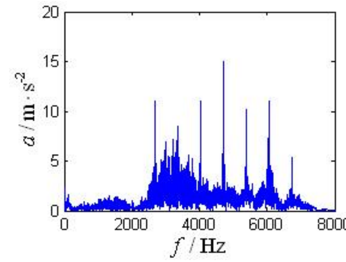

(A) Spectrum Of Broken-Teeth Signal.

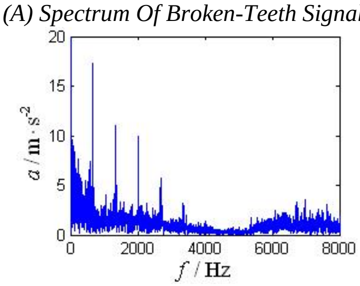

(B) Spectrum Of Processed Signal.

Fig5. Spectrum Comparison Of Broken-Teeth Signal By MUWD Method.

Comparing the above two figures, we can see that the high frequency noises are eliminated and the fault feature is obtained obviously. It is very useful in the next procedure.

Next, we calculate the sample entropy of each level. Table 1 gives the mean calculated values of five data sets in four fault conditions. From Table 1, we can see that different fault pattern has different sample entropy.

Table 1. Sample Entropy Of Different Fault Pattern.

Gear condition	SE_1	SE_2	SE_3	SE_4	SE_5
Normal	1.0222	0.5778	0.2891	0.1689	0.1192
Slight-worn	1.3418	0.6984	0.4183	0.2180	0.1250
Medium-worn	1.2994	0.6564	0.3637	0.2018	0.1194
Broken-teeth	0.9143	0.4961	0.2402	0.1387	0.1000

Table 2 gives the sample entropy of each data set in four fault conditions. Then we set the values of Table 1 as the standard fault set, we recognize different gear fault pattern by calculation the grey incidence between the fault sample and standard fault pattern.

Table 2. Sample Entropy Extracted By MUWD In Different Conditions

Gear condition	Sample	SE_1	SE_2	SE_3	SE_4	SE_5
Normal	1	1.0356	0.5925	0.2764	0.1591	0.1107
	2	1.0495	0.5873	0.2887	0.1699	0.1138
	3	0.9820	0.5645	0.2954	0.1694	0.1266
	4	1.0513	0.5882	0.3019	0.1744	0.1261
	5	0.9926	0.5567	0.2832	0.1715	0.1189
Slight-worn	1	1.3338	0.7048	0.4291	0.2263	0.1309
	2	1.3634	0.6819	0.4178	0.2091	0.1204
	3	1.3381	0.6940	0.4129	0.2179	0.1244

© 2005 - 2013 JATIT & LLS. All rights reserved·
ISSN: 1992-8645 www.jatit.org E-ISSN: 1817-3195

	4	1.3434	0.7183	0.4102	0.2179	0.1283
	5	1.3302	0.6931	0.4213	0.2190	0.1211
Medium-worn	1	1.3008	0.6437	0.3850	0.2048	0.1227
	2	1.3068	0.6722	0.3682	0.1996	0.1156
	3	1.2923	0.6634	0.3681	0.1957	0.1214
	4	1.3004	0.6474	0.3492	0.2037	0.1124
	5	1.2967	0.6553	0.3482	0.2052	0.1248
Broken-teeth	1	0.9292	0.5028	0.2295	0.1327	0.0977
	2	0.9188	0.4840	0.2501	0.1438	0.0986
	3	0.9164	0.5038	0.2336	0.1375	0.1046
	4	0.9007	0.4848	0.2417	0.1423	0.1019
	5	0.9066	0.5050	0.2462	0.1372	0.0970

Table 3 gives the final recognition results. We can see that each fault pattern has been identified by the proposed method.

Table 3. Grey Incidence Between Fault Sample And Standard Fault Pattern

Sample	Normal	Slight-worn	Medium-worn	Broken-teeth	Recognition Result
1	0.8947	0.5000	0.5961	0.6894	Normal
2	0.9247	0.4806	0.5849	0.5887	Normal
3	0.8880	0.5094	0.5467	0.5859	Normal
4	0.8870	0.5508	0.5990	0.5347	Normal
5	0.9288	0.4958	0.6034	0.6332	Normal
6	0.5560	0.9324	0.7590	0.4349	Slight-worn
7	0.6055	0.9166	0.8359	0.4483	Slight-worn
8	0.5666	0.9782	0.7898	0.4266	Slight-worn
9	0.5369	0.9409	0.7520	0.4099	Slight-worn
10	0.6018	0.9738	0.8236	0.4513	Slight-worn
11	0.6001	0.7895	0.9044	0.4249	Medium-worn
12	0.5874	0.7458	0.9469	0.4254	Medium-worn
13	0.6111	0.7485	0.9536	0.4161	Medium-worn
14	0.5552	0.6606	0.8868	0.4165	Medium-worn
15	0.5641	0.7503	0.9037	0.3867	Medium-worn
16	0.6837	0.4527	0.5095	0.9658	Broken-teeth
17	0.6676	0.4223	0.4812	0.9471	Broken-teeth
18	0.6817	0.4502	0.5097	0.9536	Broken-teeth
19	0.6706	0.4365	0.4955	0.9663	Broken-teeth
20	0.6677	0.4278	0.4861	0.9716	Broken-teeth

8. CONCLUSION

In this paper, we propose a new fault recognition method by using morphological undecimated wavelet, sample entropy and grey incidence. Its advantages are as follows:

(1) The morphological undecimated wavelet is a non-linear wavelet transform method based on morphology. It possesses both the characteristic of morphological filter in morphology and multi-resolution in wavelet transform.

(2) Based on the characteristic of difference morphological filter, the proposed method has better effectiveness in fault feature extraction of gear and the fault feature is obtained obviously.

(3) Because of the simplicity of the MUWD algorithm, the proposed method is suitable for the on-line monitoring and fault diagnosis of gear in rotating machines.

(4)Though the proposed method achieves good effectiveness in gear fault recognition, selection of the artificial intelligent recognition method is the core for future research.

ACKNOWLEDGMENT

This research is financially supported by Innovation Experimental Plot Project Fund (No. MS1102) of Honghe University.

© 2005 - 2013 JATIT & LLS. All rights reserved·
ISSN: 1992-8645 www.jatit.org E-ISSN: 1817-3195

REFRENCES:

[1] A. K. S. Jardine, D. Lin and D. Banjevic, "A review on machinery diagnostics and prognostics implementing condition-based maintenance", *Mechanical systems and signal processing*, Vol.20, 2006, pp.1483-1510.

[2] C. D. Duan, Z. J. He and H. K. Jiang, "New method for weak fault feature extraction based on second wavelet transform and its application", *Chinese Journal of Mechanical Engineering*, Vol.17, 2004, pp.543-547.

[3] J. Goutsias and H. J. A. M. Heijmans, "Nonlinear multi-resolution signal decomposition schemes-Part I: morphological pyramids", *IEEE Transactions on Image Processing*, Vol.9, 2000, pp.1862-1876.

[4] H. J. A. M. Heijmans and J. Goutsias, "Nonlinear multi-resolution signal decomposition schemes-Part II: morphological wavelets", *IEEE Transaction on Image Processing*, Vol.9, 2000, pp.1897-1913.

[5] L. J. Zhang, J. W. Xu and D. B. Yang, "Fault feature extraction to equipments using morphological wavelet denoising", *Proceedings of International Conference on Mechanical Transmissions*, Chongqing, China Beijing, Science Press, Vol.2, 2006, pp.1320-1324.

[6] J. F. Zhang, J. S. Smith and Q. H. Wu, "Morphological undecimated wavelet decomposition for fault location on power transmission lines", *IEEE Transactions on circuits and systems*, Vol.53, 2006, pp.1395-1402.

[7] B. F. Huang, L. Shen, X. J. Zhou and L. Liu, "Fault feature extraction of rolling element bearing based on morphological undecimated wavelet decomposition", *Transactions of the Chinese Society for Agriculture Machinery*, Vol.41, 2010, pp.203-207.

[8] W. B. Zhang, L. Shen, J. S. Li, Q. Cai and H. J. Wang, "Morphological undecimated wavelet decomposition for fault feature extraction of rolling element bearing", *Proceedings of the 2009 2nd International Congress on Image and Signal Processing*, 2009, pp. 4252-4258.

[9] D. E. Lake, J. S. Richman, M. P. Geriffin and J. R. Moorman, "Sample entropy analysis of neonatal heart rate variability", *Am J Physiol Regul Integr Comp Physiol*, vol. 283, 2002, pp.789-797.

[10] W. B. Zhang, L. Shen, J. S. Li, Q. Cai and H. J. Wang, "Morphological undecimated wavelet decomposition for fault feature extraction of rolling element bearing", *Proceedings of the 2009 2nd International Congress on Image and Signal Processing*, 2009, pp. 4252-4258.

[11] L. J. Zhang, J. W. Xu and J. H. Yang, "Multi-scale morphology analysis and its application to fault diagnosis", *Mechanical Systems and Signal Processing*, Vol.22, 2008, pp.597-610.

[12] R. Alcaraz, J. J. Rieta, "A review on sample entropy applications for the non-invasive analysis of atrial fibrillation electrocardiograms", *Biomedical Signal Processing and Control*, vol. 5, 2010, pp. 1-14.

[13] J. S. Richman, R. J. Moorman, "Physiological time-series analysis using approximate entropy and sample entropy", *J Physiol Heart Circ Physiol*, vol. 278, 2000, pp. 2039-2049.

[14] Y. G. Luo and C. Z. Chen, "Diagnostic analysis of grey network in rotary machinery trouble," *Compressor Blower & Fan Technology*, vol.4, 2001, pp.38-40.

[15] Y. B. Dong and X. L. Zhang, "Determination method for identification coefficient of grey relational grade and applying in mechanical faults diagnosis," *Equipment Manufacturing Technology*, vol. 3, 2008, pp.121-122, 125.

[16] Q. Zhao, J. Gao, T. F. Wu and L. Lu, "The grey theory and the preliminary probe into information acquisition technology," *Proceedings International Conference on Information Acquisition*, 2004, pp.402-404.

[17] J. Rafiee, F. Arvani, A. Harifi and M. H. Sadeghi, "Intelligent condition monitoring of a gearbox using artificial neural network", *Mechanical Systems and Signal Processing*, vol. 21, 2007, pp.1746-1754.

[18] J. Rafiee, P. W. Tse, A. Harifi and M. H. Sadeghi, "A novel technique for selecting mother wavelet function using an intelligent fault diagnosis system", *Expert Systems with Applications*, vol. 36, 2009, pp. 4862-4875.

[19] J. Rafiee and P. W. Tse, "Use of autocorrelation of wavelet coefficients for fault diagnosis", *Mechanical Systems and Signal Processing*, vol. 23, 2009, pp.1554-1572.